Astron. Astrophys. 331, 619–626 (1998)

ASTRONOMY AND ASTROPHYSICS

Extension of the effective temperature scale of giants to types later than M6

G. Perrin[1], **V. Coudé du Foresto**[1], **S.T. Ridgway**[2], **J.-M. Mariotti**[1], **W.A. Traub**[3], **N.P. Carleton**[3], **and M.G. Lacasse**[3]

[1] Observatoire de Paris, DESPA, F-92195 Meudon, France
[2] National Optical Astronomy Observatories, Tucson, AZ 85726-6732, USA
[3] Harvard-Smithsonian Center for Astrophysics, Cambridge, MA 02138, USA

Received 23 May 1997 / Accepted 27 October 1997

Abstract. Effective temperatures for nine giant stars are derived from recent diameter determinations at 2.2 μm with the FLUOR beam combiner on the IOTA interferometer. A good overlap with previous studies for stars earlier than M6 is verified. The present paper extends the temperature scale of giant stars based on direct measurements to types between M6 and M8.

Key words: techniques: interferometric – stars: atmospheres – fundamental parameters – late-type – infrared: stars

1. Introduction

The effective temperature of a star characterizes the radiometric properties of the atmosphere in a purely formal but very useful way. Effective temperatures may not in general be determined from either photometric colors or from atomic and molecular excitation, since the effective temperature is a global property and not a local property. Where a computed model atmosphere is available for a star, the effective temperature of the model will be meaningful to the extent that the model contains the required physics and boundary values. A more "direct" determination of the effective temperature, possible with little or no model dependence, may be obtained, according to the definition of effective temperature, from two observables - the apparent bolometric flux and the apparent angular diameter.

Steady improvements in techniques of optical interferometry make it possible to conduct increasingly focused studies of stellar effective temperature. Here we report an extension of the calibration of the effective temperatures of M giants to spectral types as late as M8. These will be useful as benchmarks in evaluating model atmospheres for very cool stars, and in many applications, such as correlating model luminosity functions with observed colors for composite systems.

Send offprint requests to: G. Perrin (perrin@hplyot.obspm.fr)

2. The IOTA interferometer and the FLUOR beam combiner

IOTA[1] is a Michelson type interferometer operated both in the visible and in the infrared. The interferometer is located at the Smithsonian Institution's Whipple Observatory on Mount Hopkins in Arizona. A complete and accurate description of IOTA can be found in Carleton et al. (1994). First fringes were obtained on IOTA in the near infrared in 1993 (Dyck et al. 1995).

The excellent Mt. Hopkins site, the baseline, and availability of infrared instrumentation, make IOTA an outstanding facility for study of cool stars. The first IOTA scientific results (Dyck et al. 1996a) were based on classical beam combination.

Recently, a fiber recombination unit has been installed as a focal instrument at IOTA by our group. FLUOR[2] is the heir of a prototype first operated at the McMath-Pierce solar telescope of the National Solar Observatory on Kitt Peak (Coudé du Foresto & Ridgway 1991). The recombination is achieved in the photometric K band with single-mode fluoride glass fibers. The single-mode fibers spatially filter the wavefronts corrugated by atmospheric turbulence. Phase fluctuations are thus traded against flux fluctuations which are monitored by auxiliary photometric outputs. It is then possible to directly calibrate and correct for the non-stationary atmospheric transfer function, alleviating severe inaccuracies in visibility calibrations which plague classical (multi mode) beam combiners (Coudé du Foresto et al. 1997). Progress reports on FLUOR have been presented at several conferences (see Perrin et al. 1996a, Perrin et al. 1996b). It will be described in more detail in a forthcoming paper.

3. Selection of stars

The effective temperatures of luminous, cool stars have been fairly well determined by lunar occultation to spectral types as late as M6, and additional measurements with optical and

[1] Infrared-Optical Telescope Array
[2] Fiber Linked Unit for Optical Recombination

infrared interferometry have confirmed the correctness of this calibration at the level of approximately $\pm(50-100)$ K. Extending this calibration to still cooler stars faces a number of difficulties. Though luminous, they are relatively faint in the visible, hence have not been the subject of intensive scrutiny during the classical era of stellar astronomy. They are variable in flux, color and spectral type. Their luminosities are not well known. Relatively few stars have even been classified as M8 giants.

As with many difficult problems, the best procedure is the simplest. The source list (Table 2) for the calibration program includes the "prototype" examples, that is the stars which have been selected, on basis of brightness, minimal variability, and "normal" spectrum to be primary or secondary spectral type standards (Morgan & Keenan 1973). Possible additions to this list were considered, but in each case the problems of poorer spectral type information, greater variability or lack of variability information, and increasingly uncertain extinction (for fainter stars) caused greater concern than the shortness of the list. The most immediate improvement in this list would be to add a few comparable southern stars which were not accessible from Mt. Hopkins. No doubt this list can be further improved, but possibly not without significant ancillary preparation.

In addition, the well studied stars α Boo and α Tau were observed as consistency checks against other interferometers and occultations, and the intermediate type star δ Oph was added to check the connection of our scale to previous ones for earlier stars.

Stars later than M8 were excluded. Types M9 and M10 have been used only for photometric classification of long period variables, which are known to follow a different effective temperature calibration than the normal giants (van Belle et al. 1996).

4. From interference fringes to stellar diameters

Observations were carried out at the Whipple Observatory on Mount Hopkins in October 1995, February and April 1996. In this section, we describe the observing procedure that we have adopted and the calibration process.

4.1. Observing procedure

Observing sequences unfold on a routine basis. A short-stroke delay line sweeps through the zero optical path difference (OPD thereafter) position at a speed which is computed in order to keep the OPD rate constant (the fringe frequency is typically of the order of 300 Hz). The OPD length of the sequences is about 100 μm. At the end of the scan, shutters block the beams in the two arms and a sequence of detector dark current is recorded in each output. It will be used for signal and noise calibration in the data reduction process (Coudé du Foresto et al. 1997). In regular turbulence conditions, fringes are acquired every four seconds. The standard observation of a source is a batch of 100 scans that spreads over a few minutes.

The key point of astronomical interferometry is the calibration of all losses of coherence. In order to build an estimate of the losses, observations of sources are interleaved with reference stars.

Table 1. Reference stars.

Star	Spectral type	K	Diameter (mas)
α Cet[a]	M1,5 III	-1,63	$12,08 \pm 0,60$
119 Tau[a]	M2 I	-0,90	$8,69 \pm 0,43$
μ Gem[b]	M3 III	-1,89	$13,50 \pm 0,15$
β Gem[b]	K0 III	-1,11	$7,70 \pm 0,30$
μ UMa[a]	M0 III	-0,88	$8,28 \pm 0,41$
56 Leo[a]	M5,5 III	-0,72	$8,66 \pm 0,43$
δ Vir[a]	M3 III	-1,21	$10,16 \pm 0,51$
FS Com[a]	M5 III	-0,23	$6,57 \pm 0,33$
HR 5512[a]	M5 III	-0,71	$8,28 \pm 0,41$
γ Dra[b]	K5 III	-1,34	$9,82 \pm 0,23$
γ Aql[a]	K3 II	-0,59	$6,99 \pm 0,35$
γ Sge[a]	M0 III	-0,16	$5,94 \pm 0,30$
ϵ Peg[a]	K2 I	-0,81	$7,42 \pm 0,37$
β Peg[b]	M2,5 II-III	-2,20	$16,19 \pm 0,23$

[a] photometric estimate.
[b] Di Benedetto & Rabbia (1987).

4.2. Fringe calibration

4.2.1. Diameter of reference stars

Since few stellar diameters have been measured up to now (less than one hundred), it was necessary to use indirect estimates of the diameter of reference sources in most cases. Our estimates are based on a scale of stellar diameters at $K = 0$ for giants by Dyck et al. (1996a). The diameter at a given K magnitude is derived by assuming that the surface of the star is proportional to the brightness of the star. Although the accuracy of the scale is estimated by the authors to be of the order of 10%, we suggest and adopt an accuracy of 5%. We have checked this *a priori* accuracy by comparing the photometric scale with our own results and we have found an average dispersion less than 5% between the two.

The diameters and associated accuracies of reference stars used for calibration in this paper are listed in Table 1. Stars whose diameter estimate was derived from the spectral scale are labelled with 'a'. Others, labelled with a 'b', have been directly measured, at the same wavelength, with the I2T interferometer (Di Benedetto & Rabbia 1987).

4.2.2. Computation of the transfer function

The transfer function is directly computed from the contrast of the fringes acquired on calibrators. It is the ratio between the contrast of the fringe packet and the expected visibility. Since the fringe visibility of calibrators is larger than 50%, the expected visibility is computed from a uniform disk model of the source. This will not generate an error larger than 1%. We thus measure a discrete estimate of the temporal evolution of the transfer function during the night. As the observations of scientific sources are bracketed by the observations of the reference

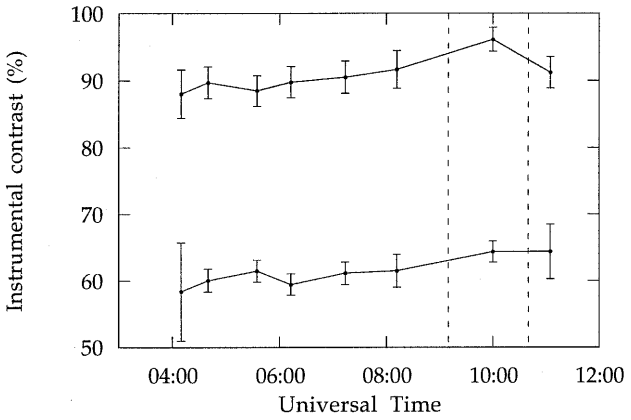

Fig. 1. FLUOR instrumental transfer function of the two interferometric outputs on 1996 April 20. $\pm 1\sigma$ error bars include the dispersion of the distribution of data points and the uncertainty on the diameter of reference stars. Vertical dashed lines are placed when the alignment of the interferometer was known to have changed.

sources it is necessary to build an estimate of the losses of coherence at the time when scientific objects are observed from non simultaneous data. To do so, the procedure is to interpolate two successive measures of the transfer function to get its evolution in the interval. We have made the assumption that this evolution is linear, that is to say that the time between two observations of reference stars is short enough so that the transfer function can be described by its first derivative.

We have represented the evolution of the (instrumental) transfer function in the two interferometric outputs in Fig.1. $\pm 1\sigma$ error bars include the dispersion of the distribution of data points and the uncertainty on the diameter of reference stars. Because the loss of coherence generated by turbulence has been removed, the average values of the instrumental contrast in the two outputs are quite high (90% and 60%). They are not equal to 100% because of residual polarization mismatches between the beams, and a degradation of the photometer time response at 300 Hz. As long as the instrumental set-up does not change, the transfer function is very stable and the fluctuations are well within the error bars. The fluctuations are smooth enough so that we can interpolate the transfer function as explained. Uncertainties on the diameter of calibrators may cause the apparent transfer function to vary but detecting this error would require a better accuracy on the tranfer function than we can achieve yet.

4.3. Visibilities and associated errors

The visibility estimates in the two outputs are the ratios of the estimates of the fringe packets contrasts and the estimates of the transfer functions. The final estimate of the visibility is the weighted mean of the visibilities in the two outputs. The final error bar is obtained by summing the reciprocals of the individual variances.

4.4. Selection of data

Since the contribution of atmospheric random phase errors to contrast error has been removed, the main source of noise on fringe contrast is detector noise. As a consequence, the accuracy on the average contrast of fringes in a batch of one hundred interferograms (the statistical accuracy) is usually better than 1% for most sources. As the final estimate of the error on the visibilities is derived from statistical accuracies, it is mandatory to check that these are meaningful. The only way to do so is to compare the simultaneous estimates of the visibility in the two outputs. If the difference between the two is consistent with the error bars then the data and the error bars are declared good. Otherwise the quality of the calibration is poor and the data are rejected. Specifically, a test is built with the residual of the fit of the two visibilities by the weighted mean. if σ_1 and σ_2 are the error bars of the two visibilities V_1 and V_2 then the residual at the optimum is:

$$\chi^2_{\rm min} = \frac{(V_1 - V_2)^2}{\sigma_1^2 + \sigma_2^2} \quad (1)$$

The data are rejected if:

$$\chi^2_{\rm min} > 3 \quad (2)$$

When observing conditions are not optimum, the instrumental transfer function evolves rapidly. The assumption of Sect. 4.2.2 on the smoothness of its variations then becomes wrong and visibilities may be badly calibrated. When conditions of observation are satisfactory, however, the rejection rate is smaller than 10%.

4.5. Stellar diameters

4.5.1. Uniform disk diameters

The data are fitted with a uniform disk model. The results of the fit in terms of uniform disk diameter are listed in the fifth column of Table 2. The error on the diameter is computed by varying the χ^2 of the fit until it increases to $\chi^2_{\rm min} + 1$. We have chosen to present two interesting examples of model fit in Fig. 2. As α Boo is one of the brightest stars that we have observed, the error bars are very small. They are nevertheless fully consistent with the dispersion of data points about the best fit curve. BK Vir, a more typical case, can also be very well fitted by a uniform disk model even though the source is fainter and the error bars are larger.

A quality factor of the adjustment is obtained by computing the ratio of the residual of the fit (χ^2_{UD}) and of the number of data points minus the number of degree of freedom in the fit, that is to say one (last column of Table 2). If this latter quantity is larger than 1 then error bars are statistically too small, by a factor equal to the square root of that quantity, and the model does not represent well the data. This occurs twice in the data and is not, therefore, representative of the general quality of the fits. It is legitimate to evaluate the quality of the calibration with the quality of the fits with a uniform disk model as most giants

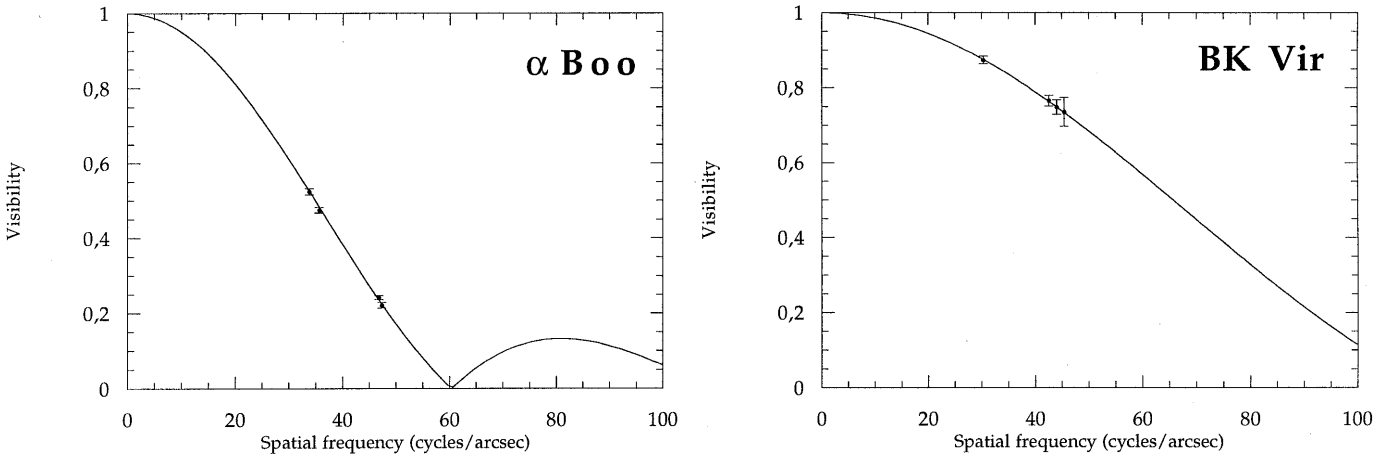

Fig. 2. Examples of fits of the FLUOR data with a uniform disk model. Left graph: α Boo, a $K = -2.95$ star. Right graph: BK Vir, a $K = -0.90$ star.

Table 2. Details of observations and results.

Star name	Spectral type	Baseline (m)	♯ data points	Uniform disk diameter (mas)	$\chi^2_{UD}/(\sharp - 1)$
α Boo	K1.5 III	15.8, 21.2	4	20.20 ± 0.08	0.25
RX Boo	M8 III	15.8, 21.2	2	18.23 ± 0.12	1.99
RS Cnc	M6.9 III	15.8, 21.2	4	14.27 ± 0.09	0.36
EU Del	M6 III	21.2	2	10.65 ± 0.25	0.07
δ Oph	M0.5 III	21.2	1	10.08 ± 0.48	-.- -
τ^4 Ser	M7.4 III	21.2	2	11.21 ± 0.18	2.40
α Tau	K5 III	21.2	2	19.75 ± 0.11	0.002
BK Vir	M7.4 III	15.8, 21.2	4	10.73 ± 0.23	0.01
SW Vir	M8 III	15.8, 21.2	3	16.81 ± 0.12	0.18

Table 3. Intrinsic colors of very cool giants.

Type	U-K	B-K	V-K	R-K	I-K	J-K	H-K	K-L	K-M
M5	9.24	7.67	6.07	3.93	2.01	1.15	0.25	0.18	-0.16
M6	9.94	8.63	6.94	4.44	2.28	1.16	0.27	0.20	-0.13
M7	10.76	9.82	8.13	4.88	2.57	1.21	0.32	0.25	0.02
M8	11.59	11.09	9.74	5.29	2.91	1.35	0.39	0.37	0.31

can be described by such a simple model at spatial frequencies smaller than the first null of the visibility function. We thus conclude that the data are well calibrated.

4.5.2. Limb-darkened disk diameters

The uniform disk diameter is a biased estimate of the real stellar diameter. The stellar limb is darker than the center of the stellar disk at wavelengths of interest here, and the averaging effect of a uniform model leads to underestimate the diameter of the star. This effect is smaller in the K band than it is in the visible. But it must be taken into account otherwise effective temperature estimates will also be biased. The bias depends upon the spatial resolution of the interferometer. We have calibrated this bias on a few stars for which we have measured high quality visibility points. To do so, we have fitted our data with limb-darkened disk models published in the literature (Manduca 1979, Scholz & Takeda 1987). In all cases the fit is of slightly better quality when the model disk is limb-darkened than when it is uniform. The average result is a ratio between the uniform and the limb-darkened disk diameters of 1.035 with a dispersion of 0.01. From the grids of published limb darkening predictions for stars in the 3000-4500 K range, we have made a best effort to estimate the ratio of limb darkening corrected diameter to uniform disk diameter. To do so, we have fitted limb darkened disk visibilities before the first null by a uniform disk model. This yields an average ratio of 1.03 with a dispersion of 0.01. Our results are thus coherent with predictions and, in the following, the real diameter of stars will be computed from the uniform disk diameter by applying the 1.035 scaling factor.

4.5.3. Check against other work

In order to intercompare angular diameters recorded at different wavelengths, it is necessary to invoke limb darkening corrections. The expected variation in apparent diameter from visible to infrared is of the order of 5% or more. Up to now, only two measurements of limb darkening have been performed: on Sirius A (Hanbury Brown et al. 1974) and on Arcturus (Quirrenbach et al. 1996). With our calibration in K we find a 20.91 ± 0.08 mas limb darkened diameter for Arcturus. This is compatible with the multi-wavelength interferometric result of Quirrenbach et al. (1996) at λ = 0.45, 0.50, 0.55, 0.70 and $0.80\,\mu m$ since they find limb darkened diameters in the range 20.78 ± 0.31 to 21.04 ± 0.05 mas.

While limb darkening for α Tau has not been directly measured, the variation of apparent diameter with color has been found to follow the expected limb darkening variation (Ridgway et al. 1982). The compilation of several multi-wavelength studies by lunar occultation yields a limb darkened diameter of 20.45 ± 0.46 mas (White & Kreidl 1984). More recently, a limb darkened diameter of 20.21 ± 0.30 was determined by Michelson interferometry observations of α Tau (Di Benedetto & Rabbia 1987). Once again, these results are compatible with our current result of 20.44 ± 0.10 mas.

5. The effective temperature scale

The fourth power of the effective temperature of a stellar object is proportional to its surface brightness according to the Stefan-Boltzmann law on the black-body radiation. This relationship can be rewritten with convenient units and convenient observable quantities:

$$T_{eff} = 7400 \left(\frac{F_{bol}}{10^{-13}\,Wcm^{-2}} \right)^{1/4} \left(\frac{1\,mas}{\oslash_{LD}} \right)^{1/2} K \qquad (3)$$

where F_{bol} is the bolometric flux in units of $10^{-13}\,Wcm^{-2}$ and $\oslash_{LD}$ is the limb darkened diameter in milli-arcseconds. The stellar interferometer has provided values for the limb darkened diameters of our sample of giant stars. No photometric observations have been carried out simultaneously with interferometric ones. It is thus necessary to estimate these fluxes from other observations. Since our sample of sources are slightly variable, error bars on the flux must take into account their variability.

5.1. Bolometric fluxes and spectral types

5.1.1. Intrinsic stellar colors and spectral types

At several points below it will be useful to have a table of the intrinsic colors of giants later than M5. We have reviewed lists of bolometrically bright giants in the spectral type range M5-M8 as classified by Morgan & Keenan (1973), Wing (1967) and Bidelman (1981). From these lists we have excluded stars of large variability, based on either a classification as long period variables, or on observed large amplitude variability, $\Delta K > 0.5$ (Two Micron Sky Survey (Gezari et al. 1993)). We have assembled available photometry for these stars, including the Two Micron Sky Survey, and numerous unpublished observations by one of the authors from Kitt Peak National Observatory. These observations have been used to estimate intrinsic colors, assuming that the brightest have no interstellar reddening, and ignoring possible circumstellar reddening. The colors are reported in Table 3.

Table 4. Photometric data and effective temperatures.

Star	V-K	I-L	A(V)	F_{bol} ($10^{-13}\,Wcm^{-2}$)	T_{eff} (K)
α Boo	2.90	1.60	-	50.4 ± 2.0	4321 ± 44
RX Boo	9.74	5.16	0.015	7.15 ± 0.46	2786 ± 46
RS Cnc	7.49	3.84	0.005	6.80 ± 1.02	3110 ± 117
EU Del	7.19	3.70	0.365	4.48 ± 0.38	3243 ± 79
δ Oph	3.94	1.85	0.100	7.40 ± 0.20	3779 ± 96
τ^4 Ser	7.56	4.09	0.034	3.80 ± 0.08	3034 ± 30
α Tau	3.67	1.53	-	33.82 ± 1.35	3947 ± 41
BK Vir	8.52	4.43	0.000	3.09 ± 0.05	2944 ± 34
SW Vir	9.66	5.06	0.039	7.35 ± 1.10	2921 ± 110

It should be noted that the spectral classifications from the sources consulted are not entirely consistent, sometimes giving different or multiple classifications for the same star. Variations of 0.5 types are typical, and may reflect both the typing uncertainty and actual variability. Consequently, on the one hand, Table 3 may be more useful statistically than for individual stars. The colors in Table 3 are given to 0.01 magnitudes to facilitate smooth interpolation - not because they are significant at this level. But, on the other hand, we have found that spectral types derived from this color table lead to more consistent results for the temperature calibration. In fact, both Morgan & Keenan (1973) and Wing (1967) spectral types are based on stellar characreristics in the visual or very near infrared domains – to $1.1\,\mu m$. Due to high continuum and line opacities, and to the temperature dependence of the exponentiel tail of the Planck function, this spectral regime is very sensitive to fluctuations in stellar conditions, whereas in the $1.2 - 4\,\mu m$ spectral region, the lower opacities reveal emission from a deeper, more stable part of the atmosphere. This suggests that a refined classification based on infrared colors computed from photometric data in bands redder than J should leave spectral types free of contamination from artifacts with basically visible characteristics that depend upon the phase when the sources are observed. The case of τ^4 Ser is very illustrative. Published spectral types are very discrepant and vary between M5 (Keenan & Mc Neil 1989) and M7 (Wing 1967). The observed colors lead to very consistent spectral types instead:

- J-K: M7.3
- H-K: M7.4
- K-L: M7.6

We have adopted as an average M7.4 which clearly confirms the later spectral type. Spectral types for sources later than M6 in Table 2 were determined with this method.

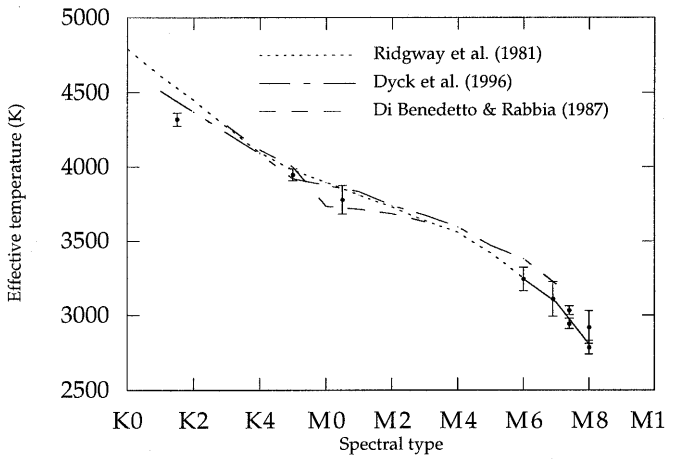

Fig. 3. Effective temperature versus spectral type. Dotted line: occultation data law (Ridgway et al. 1980). Semi continuous line: IOTA data law (Dyck et al. 1996a). Dashed line: I2T data law (Di Benedetto & Rabbia 1987). Solid line: FLUOR data law. Uncertainties on mean curves may be gauged from the difference between the various curves. The apparent discrepancy for the K1.5 III star α Boo is believed to be due to its unusual metallicity as a halo star compared to old disk stars.

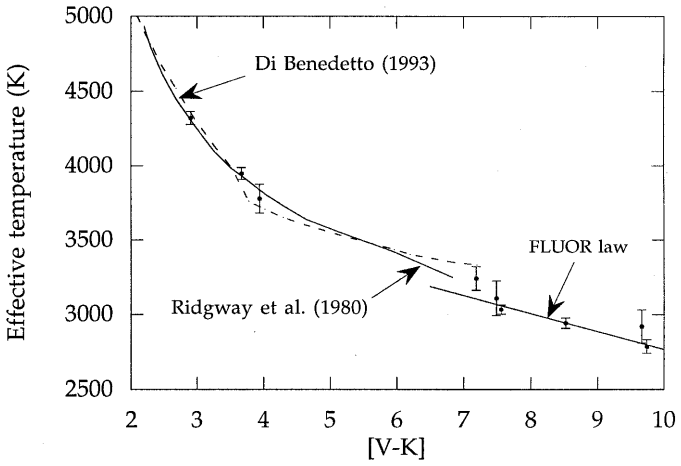

Fig. 4. Effective temperature versus V-K. Dotted line: I2T data law (Di Benedetto 1993). Curved solid line: occultation data law (Ridgway et al. 1980). Straight solid line: FLUOR data law

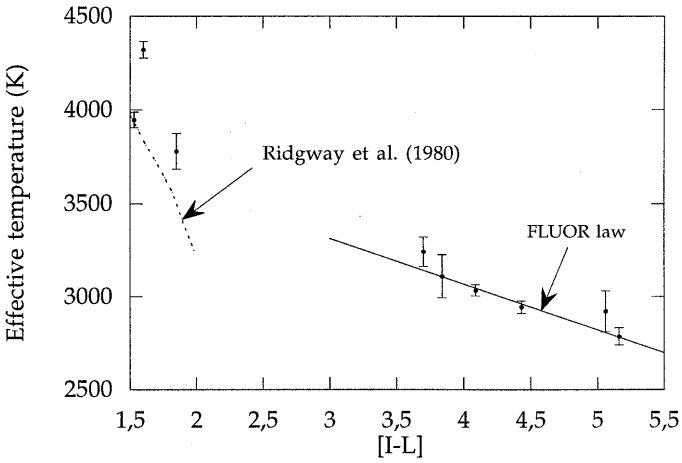

Fig. 5. Effective temperature versus I-L. Dotted line: occultation data law (Ridgway et al. 1980). Solid line: FLUOR data law

5.1.2. Bolometric fluxes

The bolometric fluxes that we have used are of different origins. Some were determined from wide band photometry (V, R, I, J, H, K, L, M) made by one of us at Kitt Peak National Observatory. No observations were made in the U and B photometric bands and some observations were missing in a few cases. Some infrared magnitudes were found in Kerschbaum & Hron (1994) and Kerschbaum (1995). Other missing magnitudes have been deduced from Table 3 for spectral types from M5 to M8, complementary to that of Johnson (1966). For two stars we have used bolometric fluxes found in the literature. For α Boo the flux has been determined by Blackwell et al. (1986) and for α Tau it has been determined by Di Benedetto & Rabbia (1987). The bolometric flux is computed from the photometry by interpolating the spectral distribution between 0.36 μm and 5 μm. The integration is extended from $\lambda = 0$ to $+\infty$ after having extrapolated the spectrum by a black body distribution matching the observed fluxes at 0.36 μm and 5 μm.

Although all sources are very bright and relatively close, it has been necessary to take interstellar reddening into account to compute the bolometric flux of all sources but α Boo and α Tau. The magnitudes of extinction in the visible are displayed in Table 4. A(V) for δ Oph and EU Del are from Fluks et al. (1994). The extinction for other stars was derived from reddening measured on nearby sources by Perry & Johnston (1982). We have assumed that the source of extinction is diffuse interstellar dust and we have used the extinction law of Mathis (1990) to compute extinction at any wavelength.

5.1.3. Error bars

Eq. 3 shows that the error on the bolometric flux contributes less to the final error on temperature than the error on the angular diameter. But this is not negligeable and we must be as careful as for the evaluation of the final error bar on diameters. Since the photometric observations were not simultaneous with interferometric observations, error bars must include the variability of the sources. To do so, we have gathered the flux calibrations listed in the Catalog of Infrared Observations (Gezari et al. 1993). For each star, we have fitted the flux measurements by a black body curve with the least square method, although the spectrum of a cool star is not a black body because of a lot of lines blanketing the entire spectrum. Fluxes were weighted with the number of observations in the corresponding photometric band. This guarantees that each photometric band contributes with the same weight. This yields a temperature and a normalization constant.

Table 5. Effective temperature scale for class III giants. Calibration for types earlier than M6 is from Ridgway et al. (1980). Types later than M6 are calibrated with the present data. Colors are from Johnson (1966) except for types later than M6 for which colors are derived from Table 3.

Spectral type	V-K	T_{eff} (K)
G8	2.20	4930
K0	2.30	4790
K1	2.48	4610
K2	2.68	4450
K3	2.96	4270
K4	3.26	4095
K5	3.52	3980
M0	3.78	3895
M1	4.02	3810
M2	4.30	3730
M3	4.64	3640
M4	5.10	3560
M5	5.96	3420
M6	6.94	3243 ± 79
M7	8.13	3087 ± 94
M8	9.74	2806 ± 42

We have estimated the average range of variation (or uncertainty) for individual wide band calibrations by the square root of the ratio of the residual at the optimum and of the number of photometric bands minus 2 (two degrees of freedom). The least square formula is normalized by this average variance to form a χ^2. The χ^2 is then varied to find the uncertainties on temperature and normalization coefficient. A Monte-Carlo Method yields the uncertainty on the bolometric flux. In all cases, this method leads to error bars that are larger than the error bars from the Kitt Peak photometry. This method has been applied to the stars later than M6 because these stars are likely to be slightly variable. Results are displayed in Table 4.

5.2. Effective temperatures

Effective temperatures are estimated with Eq. 3. Error bars are computed with a Monte-Carlo method. The estimates are presented in Table 4.

Effective temperature is plotted against spectral type in Fig. 3. The law determined from lunar occultation data (Ridgway et al. 1980)
is the dotted line and the laws determined from interferometric data, either with I2T (Di Benedetto & Rabbia 1987) or with IOTA (Dyck et al. 1996a), are the dashed and the semi continuous lines respectively. For spectral types earlier than M6 the FLUOR data are in good agreement with the mean laws except in the case of Arcturus which is about 200 K cooler than predicted by these laws for a K1.5 giant. It is probable that this discrepancy is due to the low metallicity of this halo star (Peterson et al. 1993) compared to the old disk stars.

The temperatures of stars later than M6 are found to extend well the occultation data law. The solid line on Fig. 3 is our proposed extension of the effective temperature scale with the FLUOR points. Temperature for the M6 type is that found for EU Del. Temperature for the M8 type is the average of the temperatures of SW Vir and RX Boo. Temperature for the intermediate M7 type has been established by a linear fit of the FLUOR points for types between M6 and M8. The observations of Dyck et al. (1996a) are consistent with ours, though with smaller errors and a richer selection of very cool stars, we derive a slightly different extrapolation of the occultation calibration.

Since the lunar occultation is the most consistent with the old and new data, we have chosen to merge this scale with the FLUOR scale to produce a composite law. As there is only a 7 K discrepancy between the FLUOR and the lunar occultation scale at M6, we have adopted the FLUOR calibration and its error bar for the M6 temperature. The new merged scale is tabulated in Table 5.

To be used, the spectral representation requires the knowledge of the spectral type, which may be a severe inconvenience. It may be useful to calibrate the temperature scale with a more direct observable like a color index. We have plotted effective temperatures against the [V-K] and [I-L] color indices in Figs. 4 and 5 and compared them with previous studies. Because all the sources are variable the most complex relation that can be derived from the FLUOR data is obtained with a fit by a linear law. In the [V-K] representation, our calibration is very consistent with both Ridgway et al. (1980) and Di Benedetto (1993) results. Consistency is not so obvious between the occultation data law and the FLUOR law in the [I-L] representation. Unfortunately no data are available to bridge the gap between [I-L]=2 and [I-L]=3.5 and it is difficult, with the present set of data, to comment on this discrepancy. The linear laws represented by solid lines in Figs. 4 and 5 are described by:

$$\begin{aligned} T_{\rm eff} &= -121 \pm 22 \times [V-K] + 3974 \pm 185 \\ &\text{for} \quad 7 < [V-K] < 10 \\ T_{\rm eff} &= -247 \pm 44 \times [I-L] + 4055 \pm 134 \\ &\text{for} \quad 3.5 < [I-L] < 5.5 \end{aligned} \tag{4}$$

5.3. Discussion

It is now some decades since it was realized that the effective temperatures of cool stars deviate significantly from black body fits or color temperatures. First occultation, and more recently interferometric measurements, have progressively pushed the calibration of the giant effective temperatures to later spectral types. The current extension (perhaps the final one for the "normal" giants) represents a consistent extrapolation, almost an obvious best guess, from previous work on earlier spectral types.

The known variability of the stars in our sample, in magnitude, colors and spectral type, must contribute to the scatter in Figs. 3, 4 and 5. It is interesting and perhaps significant that the color index representation has less scatter than the spectral representation. A closer look at such relations may constrain the nature of the variability, which in these stars is currently uncertain.

The errors in the concluding calibrations presented here are clearly not negligible. It may be wondered what improvement

might be expected. Of course further confirming observations, and contemporaneous spectral types and photometry, would be welcome for the current list of stars, as would an improved estimate or measure of the (small) interstellar extinction. However, at present we believe that the accuracy of the effective temperature calibration of at least the M-type stars may be approaching the limit justified by the consistency of spectral classification process, and the variability of the sources.

Furthermore, several major optical interferometer facilities are operating or under construction. It is now possible to plan scientific programs in which interferometric measurements are merely one component of an observing plan. We expect that in the future effective temperature measurements will be obtained more frequently as incidental results during the course of detailed interferometric studies of individual stars pertaining to, for example, limb darkening, evolution of surface structure, pulsation, and so forth.

6. Conclusion

The calibration of effective temperatures of normal giant stars to spectral types as cool as M8 is derived here for the first time. At present, the supporting analysis of the coolest stars with model atmospheres is challenging and still under developpment, and so this calibration from fundamental data must effectively stand on its own merits. In any event, we note that compared to previous work on slightly hotter stars, the calibration presents no surprises. Certainly it is of more than passing interest to know that the coolest giants have effective temperatures around 2800K. (As recently as 20 years ago it would have been difficult to estimate this temperature to within 500K.) It has just recently been established (Dyck et al. 1996b and van Belle et al. 1996) that many carbon stars and long period variables have significantly cooler effective temperatures. A systematic calibration of M dwarfs, which should be possible though not trivial within the next few decade, will be extremely interesting.

Acknowledgements. We thank the referee, Dr. M.S. Bessel, for his valuable comments and helpful advice. We thank the Center for Astrophysics for generous allotment of telescope time. We are also grateful to the staffs of Paris Observatory, Whipple Observatory and NOAO who helped build the FLUOR beam combiner. We especially thank Le Verre Fluoré company who provided the fibers and constant technical support. GP and VCDF are grateful to Sydney Wolff and Richard Green for their hospitality when they are visiting NOAO.

References

Bidelman W.P., 1981,
Blackwell D.E., Leggett S.K., Petford A.D., Mountain C.M., Selby M.J., 1986, MNRAS 221, 427
Carleton N.P., Traub W.A., Lacasse M.G., et al., 1994, Proc SPIE, 2200, 152
Coudé du Foresto V. , Ridgway S.T., 1991, in High resolution imaging by interferometry II, Beckers J.M. and Merkle F. Eds., Proc. ESO, 731
Coudé du Foresto V., Ridgway S.T., Mariotti J.-M., 1997, A&AS, 121, 379
Di Benedetto G., Rabbia Y., 1987, A&A 188, 114
Di Benedetto G., 1993, A&A 270, 315
Dyck H.M., Benson J.A., Carleton N.P., et al., 1995, AJ 109 (1), 378
Dyck H.M., Benson J.A., van Belle G.T., Ridgway S.T., 1996a, AJ, 111 (4), 1705
Dyck H.M., van Belle G.T., Benson J.A., 1996b, AJ 112, 294
Fluks M.A., Plez B., Thé P.S., et al., 1994, A&AS 105, 311
Gezari D.Y., Schmitz M., Pitts P.S., Mead J.M. 1993, NASA Reference Publication 1294
Hanbury Brown R., Davis J., Lake R.J.W., Thompson R.J, 1974, MNRAS 167, 475
Johnson H.L., 1966, ARA&A 4, 193
Keenan P.C., Mc Neil R.C., 1989, ApJS 71, 245
Kerschbaum F., Hron J., 1994, A&AS 106, 397
Kerschbaum F., 1995, A&AS 113, 441
Manduca A. 1979, A&AS 36, 411
Mathis J.S., 1990, ARA&A 28, 37
Morgan W.W., Keenan P.C., 1973, ARA&A 11, 29
Perrin G., Coudé du Foresto V., Ridgway S.T., et al., 1996a, Infrared Space Interferometry Workshop, in press
Perrin G., Coudé du Foresto V., Ridgway S.T., et al., 1996b, Science with the VLT Interferometer, in press
Perry C.L., Johnston L., 1982, ApJS 50, 451
Peterson R.C., Dalle Ore C.M., Kurucz R.L., 1993, ApJ 404, 333
Quirrenbach A., Mozurkewich D., Buscher D.F., Hummel C.A., Armstrong J.T., 1996, A&A 312, 160
Ridgway S.T., Joyce R.R., White N.M., Wing R.F., 1980, ApJ 235, 126
Ridgway S.T., Jacoby G.H., Joyce R.J., Siegel M.J., Wells D.C., 1982, AJ 87, 1044
Scholz M., Takeda Y., 1987, A&A 186, 200
van Belle G.T., Dyck H.M., Benson J.A., Lacasse M.G., 1996, AJ 112, 2147
White N.M., Kreidl T.J., 1984, AJ 89, 424
Wing R.F., 1967, Ph.D. thesis, University of California, Berkeley

This article was processed by the author using Springer-Verlag LaTeX A&A style file *L-AA* version 3.